

University of Groningen

Evidence of the singly Cabibbo suppressed decay $\Lambda^+ \rightarrow 0$

BESIII Collaboration; Ablikim, M.; Achasov, M.N.; Adlarson, P.; Aliberti, R.; Ai, X.C.; Amoroso, A.; Bakina, O.; Kalantar-Nayestanaki, Nasser; Kavatsyuk, Myroslav

Published in:
Physical Review D

DOI:
[10.1103/PhysRevD.109.L091101](https://doi.org/10.1103/PhysRevD.109.L091101)

IMPORTANT NOTE: You are advised to consult the publisher's version (publisher's PDF) if you wish to cite from it. Please check the document version below.

Document Version
Publisher's PDF, also known as Version of record

Publication date:
2024

[Link to publication in University of Groningen/UMCG research database](#)

Citation for published version (APA):

BESIII Collaboration, Ablikim, M., Achasov, M. N., Adlarson, P., Aliberti, R., Ai, X. C., Amoroso, A., Bakina, O., Kalantar-Nayestanaki, N., Kavatsyuk, M., & Messchendorp, J. (2024). Evidence of the singly Cabibbo suppressed decay $\Lambda^+ \rightarrow 0$. *Physical Review D*, 109(9), Article L091101 .
<https://doi.org/10.1103/PhysRevD.109.L091101>

Copyright

Other than for strictly personal use, it is not permitted to download or to forward/distribute the text or part of it without the consent of the author(s) and/or copyright holder(s), unless the work is under an open content license (like Creative Commons).

The publication may also be distributed here under the terms of Article 25fa of the Dutch Copyright Act, indicated by the "Taverne" license. More information can be found on the University of Groningen website: <https://www.rug.nl/library/open-access/self-archiving-pure/taverne-amendment>.

Take-down policy

If you believe that this document breaches copyright please contact us providing details, and we will remove access to the work immediately and investigate your claim.

Downloaded from the University of Groningen/UMCG research database (Pure): <http://www.rug.nl/research/portal>. For technical reasons the number of authors shown on this cover page is limited to 10 maximum.

Evidence of the singly Cabibbo suppressed decay $\Lambda_c^+ \rightarrow p\pi^0$

M. Ablikim *et al.**
(BESIII Collaboration)

 (Received 14 November 2023; revised 11 March 2024; accepted 22 April 2024; published 28 May 2024)

Evidence for the singly Cabibbo suppressed decay $\Lambda_c^+ \rightarrow p\pi^0$ is reported for the first time with a statistical significance of 3.7σ based on 6.0 fb^{-1} of e^+e^- collision data collected at center-of-mass energies between 4.600 and 4.843 GeV with the BESIII detector at the BEPCII collider. The absolute branching fraction of $\Lambda_c^+ \rightarrow p\pi^0$ is measured to be $(1.56_{-0.58}^{+0.72} \pm 0.20) \times 10^{-4}$. Combining with the branching fraction of $\Lambda_c^+ \rightarrow n\pi^+$, $(6.6 \pm 1.3) \times 10^{-4}$, the ratio of the branching fractions of $\Lambda_c^+ \rightarrow n\pi^+$ and $\Lambda_c^+ \rightarrow p\pi^0$ is calculated to be $3.2_{-1.2}^{+2.2}$. As an important input for the theoretical models describing the decay mechanisms of charmed baryons, our result indicates that the nonfactorizable contributions play an essential role and their interference with the factorizable contributions should not be significant. In addition, the absolute branching fraction of $\Lambda_c^+ \rightarrow p\eta$ is measured to be $(1.63 \pm 0.31_{\text{stat}} \pm 0.11_{\text{syst}}) \times 10^{-3}$.

DOI: [10.1103/PhysRevD.109.L091101](https://doi.org/10.1103/PhysRevD.109.L091101)

The hadronic weak decays of the Λ_c^+ baryon have attracted strong theoretical interest. However, until now there has been no reliable phenomenological model which could clarify the complicated underlying dynamics of charmed baryon decays. The hadronic decay amplitudes of charmed baryons generally consist of factorizable and nonfactorizable contributions. Unlike charmed mesons, the nonfactorizable contribution is not negligible compared to the factorizable ones since the W -exchange process is no longer subject to helicity and color suppression [1,2]. This makes the corresponding theoretical calculation more complicated. Moreover, the interference between the W -emission and exchange contributions remains unclear despite of the extensive studies by various phenomenological models. Therefore, experimentally investigating the nonleptonic weak hadronic decays of Λ_c^+ is highly desired, in which the two-body singly Cabibbo suppressed (SCS) decays, $\Lambda_c^+ \rightarrow n\pi^+$, $\Lambda_c^+ \rightarrow p\pi^0$, and $\Lambda_c^+ \rightarrow p\eta$, are the channels of most interest. Specifically, $\Lambda_c^+ \rightarrow n\pi^+$ and $\Lambda_c^+ \rightarrow p\pi^0$ receive the external and color-suppressed internal W -emission contributions, respectively, together with the nonfactorizable W -exchange ones. In addition, the ratio of their branching fractions (BFs) is expected to be less sensitive to the input parameters in the phenomenological models, due to the significant cancellation of the

corresponding correlated uncertainties, and is therefore effective to test the different models.

The measurements of $\Lambda_c^+ \rightarrow p\eta$ [3,4] have been demonstrated to be consistent with theoretical calculations [1,5], and the knowledge of nonfactorizable contributions has improved. However, a long-standing contradiction between experimental results and predictions on $\Lambda_c^+ \rightarrow p\pi^0$ exists. Before 2019, the SU(3) flavor (SU(3)_f) symmetry models neglected the irreducible representation $\mathcal{O}(\overline{15})$, and the predicted BFs were consistent with measurements of Cabibbo favored processes. However, the predictions on the BF of $\Lambda_c^+ \rightarrow p\pi^0$ [6,7] are significantly greater than the upper limits measured by BESIII [3] and Belle [4] experiments. Having taken the $\mathcal{O}(\overline{15})$ contribution into account, and undergone some improvements, SU(3)_f predictions updated the results for Λ_c^+ decays in 2019 [5]. Particularly, it successfully predicted the BF of $\Lambda_c^+ \rightarrow n\pi^+$, which is measured by BESIII in 2022 [8]. However, the updated prediction on BF of $\Lambda_c^+ \rightarrow p\pi^0$, $(1.3 \pm 0.7) \times 10^{-4}$, still appears to be greater than the upper limit measured by Belle, $< 8.0 \times 10^{-5}$, despite the large uncertainty. Additionally, by combining the results from Belle [4] and BESIII [8], the ratio of the BFs between $\Lambda_c^+ \rightarrow n\pi^+$ and $\Lambda_c^+ \rightarrow p\pi^0$ is calculated to be greater than 7.2 at the 90% confidence level. This result unexpectedly conflicts with most theoretical predictions, such as 2.0 with the SU(3)_f symmetry [6,7,9], 4.7 with the SU(3)_f symmetry including the contribution from $\mathcal{O}(6)$ and $\mathcal{O}(\overline{15})$ [5], 4.5 from the constituent quark model [10], and 3.5 from the dynamical calculation based on the pole model and current algebra [1]. Very recently, Ref. [11] calculated the BF of $\Lambda_c^+ \rightarrow p\pi^0$ to be $(0.51_{-0.61}^{+0.59}) \times 10^{-4}$ or

*Full author list given at end of the article.

Published by the American Physical Society under the terms of the [Creative Commons Attribution 4.0 International license](https://creativecommons.org/licenses/by/4.0/). Further distribution of this work must maintain attribution to the author(s) and the published article's title, journal citation, and DOI. Funded by SCOAP³.

TABLE I. The ΔE requirements, the ST yields in data, and the detection efficiencies of the ST and DT candidates for nine tag modes at $\sqrt{s} = 4.682$ GeV. The uncertainties of the ST yields are statistical.

	ΔE (MeV)	N_i^{ST}	ϵ_i^{ST} (%)	$\epsilon_i^{\text{DT}} p\pi^0$ (%)	$\epsilon_i^{\text{DT}} p\eta$ (%)
$\bar{p}K^+\pi^-$	(-34, 20)	$17,557 \pm 149$	47.03	22.13	20.64
$\bar{p}K_S^0$	(-20, 20)	3486 ± 62	49.61	24.66	22.43
$\bar{p}K^+\pi^-\pi^0$	(-30, 20)	2087 ± 48	41.55	21.00	19.23
$\bar{p}K_S^0\pi^0$	(-30, 20)	4159 ± 100	14.97	7.83	7.12
$\bar{p}K_S^0\pi^+\pi^-$	(-20, 20)	1545 ± 53	17.28	7.73	8.17
$\bar{\Lambda}\pi^-$	(-20, 20)	3776 ± 75	15.36	7.83	7.53
$\bar{\Lambda}\pi^-\pi^0$	(-30, 20)	1352 ± 50	18.21	7.45	7.72
$\bar{\Lambda}\pi^-\pi^+\pi^-$	(-20, 20)	1858 ± 52	12.66	5.14	5.64
$\bar{\Sigma}^0\pi^-$	(-20, 20)	1084 ± 36	20.09	11.48	10.43

$(0.16 \pm 0.09) \times 10^{-4}$, by considering the SU(3) broken or SU(3) respected effect, respectively, which is consistent with Belle's result and lower than previous SU(3)_f predictions. To clarify the aforementioned contradictions, searching for the $\Lambda_c^+ \rightarrow p\pi^0$ signal is crucial. Moreover, the study of $\Lambda_c^+ \rightarrow p\pi^0$ will definitely contribute to the interpretation of the nonfactorizable contributions and their interferences with the factorizable components.

In this paper, the first evidence of the SCS decay $\Lambda_c^+ \rightarrow p\pi^0$ is reported using e^+e^- collision data, collected by the BESIII detector at ten c.m. energies between 4.600 and 4.843 GeV, corresponding to a total integrated luminosity of 6.0 fb^{-1} [12,13]. These large data samples collected just above the $\Lambda_c^+\bar{\Lambda}_c^-$ production threshold provide a clean environment and an excellent opportunity to search for $\Lambda_c^+ \rightarrow p\pi^0$ with the double-tag approach. In addition, the decay $\Lambda_c^+ \rightarrow p\eta$ is also measured with the same approach to provide a validation. Throughout this paper, charge-conjugate modes are implicitly included.

The design and performance of the BESIII detector are described in detail in Ref. [14]. Simulated event samples are produced with a GEANT4-based [15] Monte Carlo (MC) package, which includes the geometric description [16] of the BESIII detector and the detector response. Signal MC samples of $e^+e^- \rightarrow \Lambda_c^+\bar{\Lambda}_c^-$, with $\bar{\Lambda}_c^-$ decaying to nine specific tag modes (as described below and listed in Table I), together with Λ_c^+ decaying to $p\pi^0$ or $p\eta$, are used to determine the detection efficiencies. They are generated by KKMC including the effects of initial-state radiation (ISR) and the beam energy spread. To estimate backgrounds, inclusive MC samples, which consist of $\Lambda_c^+\bar{\Lambda}_c^-$ events, $D_{(s)}^{(*)}$ production, ISR production of vector charmonium(-like) states, Bhabha scattering, $\mu^+\mu^-$, $\tau^+\tau^-$, $\gamma\gamma$ events and other inclusive hadronic processes incorporated in KKMC [17], are generated. Subsequent decays of all intermediate states are modeled with EVTGEN [18,19] using the BFs either taken from the Particle Data Group [20], when available, or modeled with LUNDCHARM [21,22]. Final state radiation from charged final state particles is incorporated using the PHOTOS package [23].

This work is carried out by the double-tag (DT) method. First, we select a data sample of the process $e^+e^- \rightarrow \Lambda_c^+\bar{\Lambda}_c^-$, called the single-tag (ST) sample, by tagging a $\bar{\Lambda}_c^-$ baryon with one of the nine exclusive hadronic decay modes, as listed in the first column of Table I. Then, we search for the signal decays $\Lambda_c^+ \rightarrow p\pi^0$ and $\Lambda_c^+ \rightarrow p\eta$ in the system recoiling against the ST $\bar{\Lambda}_c^-$ candidates, referred to as the DT sample hereafter.

Charged tracks, photon candidates as well as the intermediate π^0 , K_S^0 , $\bar{\Lambda}$, and $\bar{\Sigma}^0$ states are selected and reconstructed using the same criteria described in detail in Ref. [8]. In addition, the kaon candidate is now required to have a particle identification (PID) probability to be a kaon greater than 0.0005, in order to suppress background with pions misidentified as kaons. PID for charged tracks combines measurements of the energy deposited in the helium-based multilayer drift chamber, dE/dx , and the flight time from the time-of-flight system to form likelihoods $\mathcal{L}(h)$ ($h = p, K, \pi$) for each hadron hypothesis. Two variables, the energy difference, $\Delta E = E_{\bar{\Lambda}_c^-} - E_{\text{beam}}$, and the beam energy constrained mass $M_{\text{BC}} = \sqrt{E_{\text{beam}}^2/c^4 - |\vec{p}_{\bar{\Lambda}_c^-}|^2/c^2}$, are adopted to identify the ST $\bar{\Lambda}_c^-$ candidates, where E_{beam} is the beam energy, and $E_{\bar{\Lambda}_c^-}$ and $\vec{p}_{\bar{\Lambda}_c^-}$ are the energy and momentum of the $\bar{\Lambda}_c^-$ candidate, respectively. The tagged candidates are selected with the minimum $|\Delta E|$ among all the candidates, and are required to satisfy the ΔE requirements listed in the second column of Table I. To avoid cross feed from the other ST modes, the same requirements as in Ref. [24] are applied for the $\bar{\Lambda}_c^- \rightarrow \bar{p}K_S^0\pi^0$, $\bar{\Lambda}_c^- \rightarrow \bar{p}K_S^0\pi^+\pi^-$ and $\bar{\Lambda}\pi^-\pi^+\pi^-$ modes.

The ST yields are extracted by performing unbinned maximum likelihood fits to the corresponding M_{BC} distributions in the range $(2.2, E_{\text{beam}}) \text{ GeV}/c^2$. In the fit, the signal shape is modeled by the M_{BC} spectrum extracted from the signal MC sample convolved with a Gaussian function to compensate for the resolution difference between the data and the MC simulation. The background is described by an ARGUS function [25] with the endpoint

parameter fixed to the corresponding E_{beam} . The detection efficiencies of ST candidates are estimated with MC samples of $e^+e^- \rightarrow \Lambda_c^+ \bar{\Lambda}_c^-$ with $\bar{\Lambda}_c^-$ decaying to one of the nine tag modes and Λ_c^+ decaying generically to all possible final states. The ST yields and efficiencies at $\sqrt{s} = 4.682$ GeV are shown in Table I. The results, including the ST yields and efficiencies for the other nine c.m. energies, and the fits for all c.m. energies are summarized in the Supplemental Material [26]. The total ST yield for all ten c.m. energies is $119398 \pm 413_{\text{stat}}$ events.

The signal decays $\Lambda_c^+ \rightarrow p\pi^0$ and $\Lambda_c^+ \rightarrow p\eta$ are searched for in the remaining objects recoiling against the ST $\bar{\Lambda}_c^-$ candidates. The selection criteria for charged tracks and photons are the same as those in the ST selection. The distance of the closest approach to the interaction point along the beam direction is required to be less than 10 cm and 20 cm for tight and loose tracks, respectively [8]. In addition, the corresponding distance perpendicular to the beam direction is required to be less than 1 cm for a tight track. To suppress multitrack backgrounds, there must be only one tight track, identified as a proton, and no loose tracks. In order to eliminate noise created by \bar{p} in the electromagnetic calorimeter, photons are required to be separated from \bar{p} with an opening angle greater than 30° . To improve its purity, the photon candidates are further required to have their lateral moment in the range of (0.05,0.40) and have an $E_{3 \times 3}/E_{5 \times 5}$ greater than 0.85, where $E_{3 \times 3}$ ($E_{5 \times 5}$) is the shower energy summed over a 3×3 (5×5) group of crystals around the central seed crystal. Events with at least two photon candidates are kept for further analysis.

The signal candidate is reconstructed with the selected proton and two photons. For those events with multiple candidates (roughly 10% of the total events), only the one with the minimum energy difference $|\Delta E_{p2\gamma}| = |E_p + E_{\gamma 1} + E_{\gamma 2} - E_{\text{beam}}|$ is kept, where E_p and $E_{\gamma 1/2}$ are the energies of the proton and two photons, respectively. The criterion $-0.080 < \Delta E_{p2\gamma} < 0.035$ GeV, optimized by using the inclusive and signal MC samples, is applied to further suppress the background.

A clear Λ peak is observed in the invariant mass distribution of the proton from the signal side and a π^- from the ST side. Thus, an event is rejected if the invariant mass of any such combination of p and π^- lies within (1.111, 1.121) GeV/ c^2 . Similarly, an ω signal is seen in the invariant mass distribution of the π^0 from the signal side and $\pi^+\pi^-$ pairs from ST side. Events with an invariant mass of any such combination within (0.733, 0.833) GeV/ c^2 are also rejected.

The signal decays are examined by $M_{\text{BC}}^{\text{ST}}$ of the tag side, and $M_{\gamma\gamma}$ and $M_{\text{BC}}^{p2\gamma}$ of the signal side. Here, $M_{\gamma\gamma}$ is the invariant mass of two photons, and $M_{\text{BC}}^{\text{ST}}$ and $M_{\text{BC}}^{p2\gamma}$ are the beam energy constrained masses of the ST $\bar{\Lambda}_c^-$ and signal candidate. The combined distribution of $M_{\gamma\gamma}$

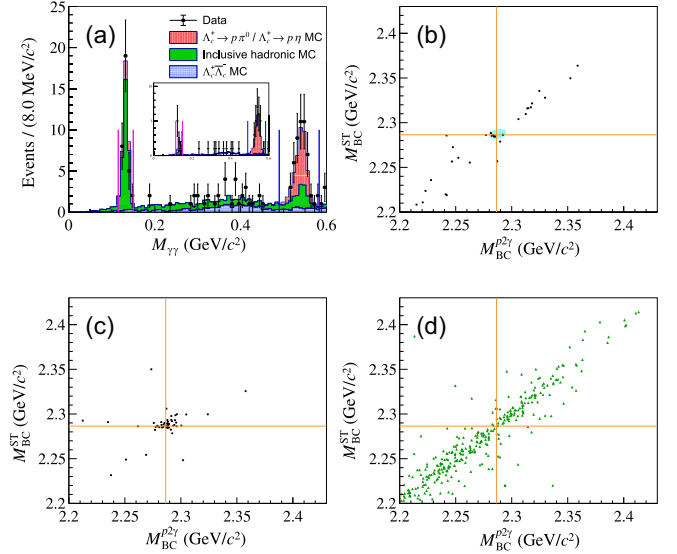


FIG. 1. The invariant mass distribution of $\gamma\gamma$ (a). The subfigure shows the $M_{\gamma\gamma}$ distribution in the 2D M_{BC} signal region ($M_{\text{BC}}^{\text{ST}} \in [2.280, 2.295]$ GeV/ c^2 and $M_{\text{BC}}^{p2\gamma} \in [2.280, 2.295]$ GeV/ c^2). The scatter plots of $M_{\text{BC}}^{p2\gamma}$ versus $M_{\text{BC}}^{\text{ST}}$ for the candidate events with $M_{\gamma\gamma}$ within the (b) π^0 signal region of data, (c) η signal region of data, and (d) π^0 signal region of inclusive hadronic background MC sample with a total integrated luminosity of ten times of data. The blue oval in (b) represents the one-sigma resolution of the signal MC. The orange lines denote the nominal Λ_c mass.

from the ten c.m. energies is shown in Fig. 1(a), where both π^0 and η signals are observed. The π^0 and η signal regions are defined as (0.115, 0.150) GeV/ c^2 and (0.490, 0.583) GeV/ c^2 , as indicated by the regions between two magenta and blue lines, respectively. The background in region (0.17, 0.47) GeV/ c^2 is dominated by the decays $\Lambda_c^+ \rightarrow \Sigma^+(\rightarrow p\pi^0)\pi^0$ and $\Lambda_c^+ \rightarrow pK_S^0(\rightarrow \pi^0\pi^0)$. The η signal is dominated by $\Lambda_c^+ \rightarrow p\eta$; however, the π^0 signal suffers from a large contamination from inclusive hadronic processes.

The distribution of $M_{\text{BC}}^{\text{ST}}$ versus $M_{\text{BC}}^{p2\gamma}$ and their projections for the candidate events with $M_{\gamma\gamma}$ in the π^0 signal region, are shown in Figs. 1(b), 2(a), and 2(b), respectively. The events accumulating around the intersection of $M_{\text{BC}}^{\text{ST}} = M_{\Lambda_c}$ and $M_{\text{BC}}^{p2\gamma} = M_{\Lambda_c}$ provide evidence for $\Lambda_c^+ \rightarrow p\pi^0$ (here, M_{Λ_c} denotes the known Λ_c mass [20]). Similarly, Figs. 1(c), 2(c), and 2(d) illustrate the distribution of $M_{\text{BC}}^{\text{ST}}$ versus $M_{\text{BC}}^{p2\gamma}$ and their projections with $M_{\gamma\gamma}$ in the η signal region, respectively, where the $\Lambda_c^+ \rightarrow p\eta$ signal can be clearly seen. The distribution of the inclusive hadronic background MC sample in the π^0 signal region is shown in Fig. 1(d), where no accumulation of events in the vicinity of the intersection point is observed. As is shown in Fig. 1, nine events are observed in the one-sigma signal region, while the inclusive hadronic MC sample predicts about

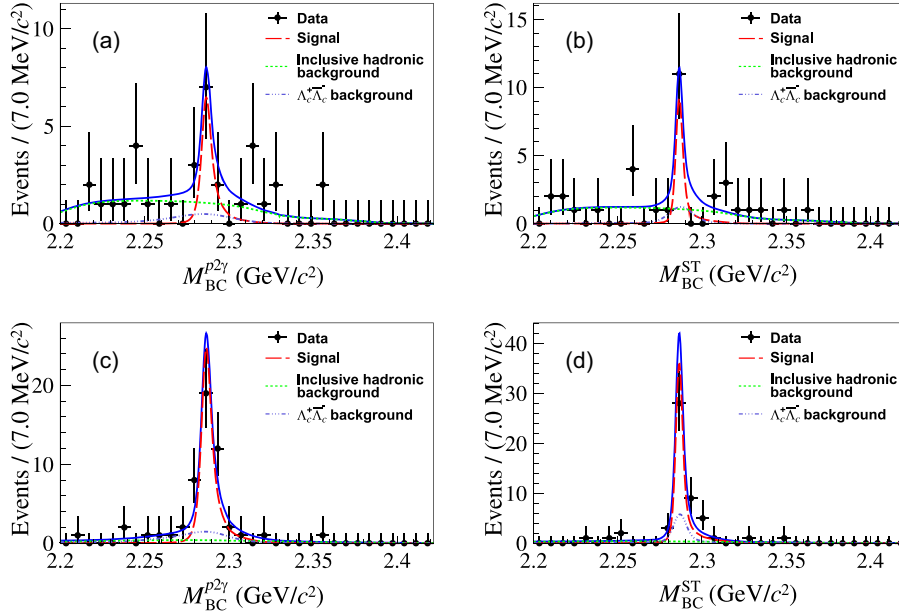


FIG. 2. The 1D projections of the 2D fits for $\Lambda_c^+ \rightarrow p\pi^0$ and $\Lambda_c^+ \rightarrow p\eta$, where (a) and (b) are $M_{BC}^{p2\gamma}$ and M_{BC}^{ST} for $\Lambda_c^+ \rightarrow p\pi^0$, and (c) and (d) are the corresponding plots for $\Lambda_c^+ \rightarrow p\eta$. The black dots denote data, and the blue solid curves are the sum of the fit functions. The signal is illustrated by the red dashed curves, while background from the inclusive hadronic events and the nonsignal $e^+e^- \rightarrow \Lambda_c^+\bar{\Lambda}_c^-$ events are denoted by the green and blue dashed curves, respectively.

0.7 events for the data equivalent luminosity. The distribution of the $\Lambda_c^+\bar{\Lambda}_c^-$ background MC sample in the π^0 signal region as well as those in the η signal region are given in the Supplemental Material [26].

The BFs of the decays $\Lambda_c^+ \rightarrow p\eta$ and $\Lambda_c^+ \rightarrow p\pi^0$ are obtained by performing a simultaneous unbinned maximum likelihood fit on the two-dimensional (2D) distribution of $M_{BC}^{p2\gamma}$ versus M_{BC}^{ST} among the ten data samples with different c.m. energies. In the fit, the signal is modeled with an MC-simulated shape convolved with Gaussian functions (for $M_{BC}^{p2\gamma}$ and M_{BC}^{ST} , individually) representing the resolution difference between data and MC simulation. The mean and width of the Gaussian functions are extracted from the fit to a control sample of $\Lambda_c^+ \rightarrow pK^-\pi^+\pi^0$. The inclusive hadronic background is modeled with the product of two ARGUS functions and a Student's t -distribution describing the dispersion of the inclusive hadronic background in the diagonal direction. Details of the background functions as well as the free and fixed parameters are given in the Supplemental Material [26]. The background from nonsignal $e^+e^- \rightarrow \Lambda_c^+\bar{\Lambda}_c^-$ events is modeled with the inclusive MC samples. The same decay BF is shared among the different c.m. energies in the simultaneous fit with the relation

$$\mathcal{B} \cdot \sum_i (\epsilon_i^{\text{DT}} \cdot N_i^{\text{ST}} / \epsilon_i^{\text{ST}}) + N_{\text{bkg}} = N_{\text{total}}, \quad (1)$$

where the subscript i represents the i th ST mode, N_{total} and N_{bkg} denote the total event yields and backgrounds, and ϵ_i^{DT}

represents the DT detection efficiencies, which are extracted from the DT signal MC samples. The quantities N_i^{ST} , ϵ_i^{ST} and ϵ_i^{DT} used in the 2D fit are summarized in Table I for the data sample with c.m. energy $\sqrt{s} = 4.682$ GeV, and in the Supplemental Material [26] for the other nine c.m. energies.

The simultaneous fit yields the BFs $\mathcal{B}(\Lambda_c^+ \rightarrow p\eta) = (1.63 \pm 0.31) \times 10^{-3}$ and $\mathcal{B}(\Lambda_c^+ \rightarrow p\pi^0) = (1.56^{+0.72}_{-0.58}) \times 10^{-4}$, which correspond to the signal yields of 34.7 ± 6.6 and $8.8^{+4.0}_{-3.3}$ events, respectively, for the ten total c.m. energies. The projections of $M_{BC}^{p2\gamma}$ and M_{BC}^{ST} are shown in Fig. 2, where the fit curves describe the data well. The statistical significances, which are estimated from the change of likelihood values and the change of degrees of freedom with and without the signal function included in the fit, are 6.9σ and 3.8σ for $\Lambda_c^+ \rightarrow p\eta$ and $\Lambda_c^+ \rightarrow p\pi^0$, respectively.

The systematic uncertainties for the BF measurement include those associated with the ST and DT yields, the detection efficiencies from the signal side, the BFs of $\pi^0 \rightarrow \gamma\gamma$ and $\eta \rightarrow \gamma\gamma$, and MC statistics.

The uncertainties in the ST detection efficiencies are canceled by the DT method. The uncertainty associated with DT efficiencies, ϵ_i^{DT} , has several sources. Systematic effects due to the proton tracking and PID efficiencies are estimated using the control sample $J/\psi \rightarrow p\bar{p}\pi^+\pi^-$ [8] and give 1.0% and 1.0%, respectively. The uncertainties originating from the photon reconstruction efficiency and shower shape requirements are studied by the control

sample $J/\psi \rightarrow \rho^0 \pi^0 \rightarrow \pi^+ \pi^- \pi^0$ [27], where 1.0% and 0.5% per photon are obtained, respectively. The uncertainty from the requirement of the opening angle between photon and antiproton is 0.5% per photon, which is obtained by studying a control sample of $J/\psi \rightarrow p \bar{p} \pi^0$. A Barlow test [28] is carried out to examine the uncertainties due to the mass window requirements vetoing the backgrounds associated with Λ and ω , where no significant systematic deviation is observed. The systematic uncertainty from the ΔE requirement on the signal side is found to be 0.3% by studying the control samples of modes $\Lambda_c^+ \rightarrow p K^- \pi^+ \pi^0$ and $\Lambda_c^+ \rightarrow \Lambda \pi^+ \pi^0$. The uncertainty due to the signal MC model is taken as 0.4% [29]. Uncertainties from the BFs of $\eta \rightarrow \gamma\gamma$ and $\pi^0 \rightarrow \gamma\gamma$ are taken from PDG [20]. The uncertainty due to the MC statistics is 0.1%. The ST yields contribute to the uncertainty of BF by 0.5% [8]. The uncertainties due to the DT yield extraction are 5.7% and 12.4% for $\Lambda_c^+ \rightarrow p\eta$ and $\Lambda_c^+ \rightarrow p\pi^0$, respectively, which is the quadratic sum of the individual changes of signal yields obtained from the alternative fits by changing the fixed parameters in the shapes of the signal and background by $\pm 1\sigma$.

Assuming all sources of the uncertainties are uncorrelated, the quadratic sums of the different contributions are taken as the total uncertainties. For $\Lambda_c^+ \rightarrow p\eta$ and $\Lambda_c^+ \rightarrow p\pi^0$, the total systematic uncertainties become 6.4% and 12.8%, respectively. Alternative fits of changing the fixed parameters of background shape with $\pm 1\sigma$ deviation are performed individually, and corresponding fits with the signal removed are performed. The most conservative significance among all changes is taken as the statistical significance accounting for the systematic uncertainty, and the significance is 3.7σ .

In summary, based on e^+e^- collision data samples with a total integrated luminosity of 6.0 fb^{-1} collected at c.m. energies between 4.600 and 4.843 GeV with the BESIII detector, the SCS decays $\Lambda_c^+ \rightarrow p\pi^0$ and $\Lambda_c^+ \rightarrow p\eta$ are measured using a DT method. Evidence is obtained for the decay $\Lambda_c^+ \rightarrow p\pi^0$, with a statistical significance of 3.7σ and a decay BF of $(1.56_{-0.58}^{+0.72} \pm 0.20) \times 10^{-4}$. The BF of $\Lambda_c^+ \rightarrow p\eta$ is measured as $(1.63 \pm 0.31_{\text{stat}} \pm 0.11_{\text{syst}}) \times 10^{-3}$, consistent with previous results [3,4,29]. The $\mathcal{B}(\Lambda_c^+ \rightarrow p\pi^0)$ result distinctly exceeds the upper limit measured by the Belle experiment. Taking $\mathcal{B}(\Lambda_c^+ \rightarrow n\pi^+) = (6.6 \pm 1.3) \times 10^{-4}$ [8], the ratio of the BFs between $\Lambda_c^+ \rightarrow n\pi^+$ and $\Lambda_c^+ \rightarrow p\pi^0$ is calculated to be $3.2_{-1.2}^{+2.2}$, where 3.2 denotes the most probable value, and the upper and lower errors cover the 68% confidence interval. This value is obtained by generating toy MC samples and forming a Probability Density Function of the ratio. The detailed method is given in the Supplemental Material [26]. This ratio is consistent with the majority of phenomenological predictions [1,5–7,9,10]. More importantly, not only the ratio but also the individual BFs of $\Lambda_c^+ \rightarrow p\pi^0$ and

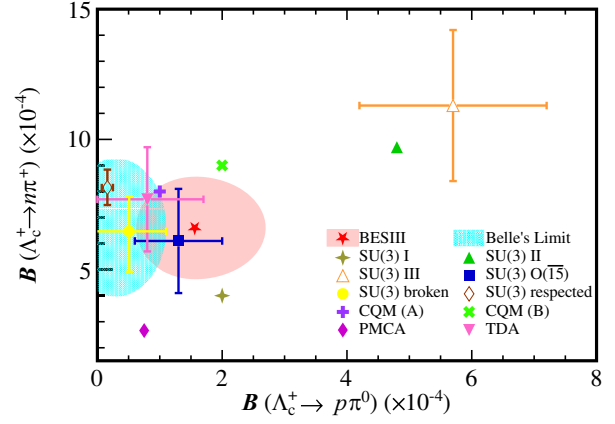


FIG. 3. Distribution of BF of $\Lambda_c^+ \rightarrow n\pi^+$ versus BF of $\Lambda_c^+ \rightarrow p\pi^0$. The red star denotes the results measured by this work, and the pink contour corresponds to the 68% confidence interval of the results. The cyan shadowed area shows the upper limit at 90% confidence level from Belle [4]. The BF of $\Lambda_c^+ \rightarrow n\pi^+$ of both two shadowed area is from BESIII [8]. Other symbols stand for the phenomenological predictions: $SU(3)_f$ symmetry (SU(3) I refers to Ref. [9], SU(3) II refers to Ref. [7], and SU(3) III refers to Ref. [6]), SU(3) including the contribution from $\mathcal{O}(6)$ and $\mathcal{O}(\overline{15})$ (referred to as SU(3) $\mathcal{O}(\overline{15})$) [5], SU(3) broken and respected [11], constituent quark model (CQM) [10] with two predictions (A) and (B), dynamical calculation based on the pole model and current algebra (PMCA) [1], and topological-diagram approach (TDA) [30].

$\Lambda_c^+ \rightarrow n\pi^+$ agree with the calculation of $SU(3)_f$ symmetry including the contributions from both $\mathcal{O}(6)$ and $\mathcal{O}(\overline{15})$ [5], which indicates that the nonfactorizable contributions play an essential role in these two decays and their interference with the factorizable contributions should not be significant. The comparisons between the measurement results with Belle's upper limit and phenomenological predictions are shown in Fig. 3. Our results provide important input for these phenomenological models and contribute to the distinction between them.

The BESIII Collaboration thanks the staff of BEPCII, the IHEP computing center and the supercomputing center of the University of Science and Technology of China (USTC) for their strong support. The authors are grateful to Yu-Kuo Hsiao for enlightening discussions. This work is supported in part by National Key R&D Program of China under Contracts No. 2020YFA0406400 and No. 2020YFA0406300; National Natural Science Foundation of China (NSFC) under Contracts No. 11335008, No. 11625523, No. 12035013, No. 11705192, No. 11950410506, No. 12061131003, No. 12105276, No. 12122509, No. 11635010, No. 11735014, No. 11835012, No. 11935015, No. 11935016, No. 11935018, No. 11961141012, No. 12022510, No. 12025502, No. 12035009, No. 12192260, No. 12192261, No. 12192262,

No. 12192263, No. 12192264, No. 12192265, No. 12221005, No. 12225509, No. 12235017, and No. 12005311; China Postdoctoral Science Foundation under Contracts No. 2019M662152, No. 2020T130636; the Fundamental Research Funds for the Central Universities, University of Science and Technology of China under Contract No. WK2030000053; the Chinese Academy of Sciences (CAS) Large-Scale Scientific Facility Program; the CAS Center for Excellence in Particle Physics (CCEPP); Joint Large-Scale Scientific Facility Funds of the NSFC and CAS under Contracts No. U1732263, No. U1832103, No. U2032111, No. U1832207; CAS Key Research Program of Frontier Sciences under Contracts No. QYZDJ-SSW-SLH003, and No. QYZDJ-SSW-SLH040; 100 Talents Program of CAS; The Institute of Nuclear and Particle Physics (INPAC) and Shanghai Key Laboratory for Particle Physics and Cosmology; ERC under Contract No. 758462; European Union's Horizon

2020 research and innovation programme under Marie Skłodowska-Curie Grant Agreement under Contract No. 894790; German Research Foundation DFG under Contract No. 455635585, Collaborative Research Center CRC 1044, FOR5327, GRK 2149; Istituto Nazionale di Fisica Nucleare, Italy; Ministry of Development of Turkey under Contract No. DPT2006K-120470; National Research Foundation of Korea under Contract No. NRF-2022R1A2C1092335; National Science and Technology fund of Mongolia; National Science Research and Innovation Fund (NSRF) via the Program Management Unit for Human Resources & Institutional Development, Research and Innovation of Thailand under Contract No. B16F640076; Polish National Science Centre under Contract No. 2019/35/O/ST2/02907; The Swedish Research Council; and U.S. Department of Energy under Contract No. DE-FG02-05ER41374.

-
- [1] H.-Y. Cheng, X.-W. Kang, and F. Xu, *Phys. Rev. D* **97**, 074028 (2018).
- [2] H.-Y. Cheng, *Front. Phys.* **10**, 101406 (2015).
- [3] M. Ablikim *et al.* (BESIII Collaboration), *Phys. Rev. D* **95**, 111102 (2017).
- [4] S. X. Li *et al.* (Belle Collaboration), *Phys. Rev. D* **103**, 072004 (2021).
- [5] C.-Q. Geng, C.-W. Liu, and T.-H. Tsai, *Phys. Lett. B* **790**, 225 (2019).
- [6] C. Q. Geng, Y. K. Hsiao, C.-W. Liu, and T.-H. Tsai, *Phys. Rev. D* **97**, 073006 (2018).
- [7] C.-D. Lü, W. Wang, and F.-S. Yu, *Phys. Rev. D* **93**, 056008 (2016).
- [8] M. Ablikim *et al.* (BESIII Collaboration), *Phys. Rev. Lett.* **128**, 142001 (2022).
- [9] K. K. Sharma and R. C. Verma, *Phys. Rev. D* **55**, 7067 (1997).
- [10] T. Uppal, R. C. Verma, and M. P. Khanna, *Phys. Rev. D* **49**, 3417 (1994).
- [11] H. Zhong, F. Xu, Q. Wen, and Y. Gu, *J. High Energy Phys.* **02** (2023) 235.
- [12] M. Ablikim *et al.* (BESIII Collaboration), *Chin. Phys. C* **46**, 113002 (2022).
- [13] M. Ablikim *et al.* (BESIII Collaboration), *Chin. Phys. C* **46**, 113003 (2022).
- [14] M. Ablikim *et al.* (BESIII Collaboration), *Nucl. Instrum. Method Phys. Res. Sect. A* **614**, 345 (2010).
- [15] S. Agostinelli *et al.* (GEANT4 Collaboration), *Nucl. Instrum. Method Phys. Res. Sect. A* **506**, 250 (2003).
- [16] K.-X. Huang *et al.*, *Nucl. Sci. Tech.* **33**, 142 (2022).
- [17] S. Jadach, B. F. L. Ward, and Z. Was, *Phys. Rev. D* **63**, 113009 (2001).
- [18] D. J. Lange, *Nucl. Instrum. Method Phys. Res. Sect. A* **462**, 152 (2001).
- [19] R. G. Ping, *Chin. Phys. C* **32**, 599 (2008).
- [20] R. L. Workman *et al.* (Particle Data Group), *Prog. Theor. Exp. Phys.* **2022**, 083C01 (2022).
- [21] J. C. Chen, G. S. Huang, X. R. Qi, D. H. Zhang, and Y. S. Zhu, *Phys. Rev. D* **62**, 034003 (2000).
- [22] R.-L. Yang, R.-G. Ping, and H. Chen, *Chin. Phys. Lett.* **31**, 061301 (2014).
- [23] E. Richter-Was, *Phys. Lett. B* **303**, 163 (1993).
- [24] M. Ablikim *et al.* (BESIII Collaboration), *Phys. Rev. Lett.* **120**, 132001 (2018).
- [25] H. Albrecht *et al.* (ARGUS Collaboration), *Phys. Lett. B* **241**, 278 (1990).
- [26] See Supplemental Material at <http://link.aps.org/supplemental/10.1103/PhysRevD.109.L091101> for additional details, including the single-tag fit results, yields and efficiencies, the double-tag efficiencies, the scatter plots of inclusive background MC samples in signal region, the detailed description of inclusive hadronic background model in the fit, as well as the method to obtain the ratio between branching fractions of $\Lambda_c^+ \rightarrow n\pi^+$ and $\Lambda_c^+ \rightarrow p\pi^0$.
- [27] M. Ablikim *et al.* (BESIII Collaboration), *Phys. Rev. D* **81**, 052005 (2010).
- [28] R. Barlow, [arXiv:hep-ex/0207026](https://arxiv.org/abs/hep-ex/0207026).
- [29] M. Ablikim *et al.* (BESIII Collaboration), *J. High Energy Phys.* **11** (2023) 137.
- [30] H. J. Zhao, Y.-L. Wang, Y. K. Hsiao, and Y. Yu, *J. High Energy Phys.* **02** (2020) 165.

M. Ablikim,¹ M. N. Achasov,^{5,b} P. Adlarson,⁷⁴ X. C. Ai,⁸⁰ R. Aliberti,³⁵ A. Amoroso,^{73a,73c} M. R. An,³⁹ Q. An,^{70,57} Y. Bai,⁵⁶ O. Bakina,³⁶ I. Balossino,^{29a} Y. Ban,^{46,g} V. Batozskaya,^{1,44} K. Begzsuren,³² N. Berger,³⁵ M. Berlowski,⁴⁴ M. Bertani,^{28a} D. Bettoni,^{29a} F. Bianchi,^{73a,73c} E. Bianco,^{73a,73c} A. Bortone,^{73a,73c} I. Boyko,³⁶ R. A. Briere,⁶ A. Brueggemann,⁶⁷ H. Cai,⁷⁵ X. Cai,^{1,57} A. Calcaterra,^{28a} G. F. Cao,^{1,62} N. Cao,^{1,62} S. A. Cetin,^{61a} J. F. Chang,^{1,57} T. T. Chang,⁷⁶ W. L. Chang,^{1,62} G. R. Che,⁴³ G. Chelkov,^{36,a} C. Chen,⁴³ Chao Chen,⁵⁴ G. Chen,¹ H. S. Chen,^{1,62} M. L. Chen,^{1,57,62} S. J. Chen,⁴² S. M. Chen,⁶⁰ T. Chen,^{1,62} X. R. Chen,^{31,62} X. T. Chen,^{1,62} Y. B. Chen,^{1,57} Y. Q. Chen,³⁴ Z. J. Chen,^{25,h} W. S. Cheng,^{73c} S. K. Choi,¹¹ X. Chu,⁴³ G. Cibinetto,^{29a} S. C. Coen,⁴ F. Cossio,^{73c} J. J. Cui,⁴⁹ H. L. Dai,^{1,57} J. P. Dai,⁷⁸ A. Dbeyssi,¹⁸ R. E. de Boer,⁴ D. Dedovich,³⁶ Z. Y. Deng,¹ A. Denig,³⁵ I. Denysenko,³⁶ M. Destefanis,^{73a,73c} F. De Mori,^{73a,73c} B. Ding,^{65,1} X. X. Ding,^{46,g} Y. Ding,⁴⁰ Y. Ding,³⁴ J. Dong,^{1,57} L. Y. Dong,^{1,62} M. Y. Dong,^{1,57,62} X. Dong,⁷⁵ M. C. Du,¹ S. X. Du,⁸⁰ Z. H. Duan,⁴² P. Egorov,^{36,a} Y. H. Y. Fan,⁴⁵ Y. L. Fan,⁷⁵ J. Fang,^{1,57} S. S. Fang,^{1,62} W. X. Fang,¹ Y. Fang,¹ R. Farinelli,^{29a} L. Fava,^{73b,73c} F. Feldbauer,⁴ G. Felici,^{28a} C. Q. Feng,^{70,57} J. H. Feng,⁵⁸ K. Fischer,⁶⁸ M. Fritsch,⁴ C. Fritsch,⁶⁷ C. D. Fu,¹ J. L. Fu,⁶² Y. W. Fu,¹ H. Gao,⁶² Y. N. Gao,^{46,g} Yang Gao,^{70,57} S. Garbolino,^{73c} I. Garzia,^{29a,29b} P. T. Ge,⁷⁵ Z. W. Ge,⁴² C. Geng,⁵⁸ E. M. Gersabeck,⁶⁶ A. Gilman,⁶⁸ K. Goetzen,¹⁴ L. Gong,⁴⁰ W. X. Gong,^{1,57} W. Gradl,³⁵ S. Gramigna,^{29a,29b} M. Greco,^{73a,73c} M. H. Gu,^{1,57} C. Y. Guan,^{1,62} Z. L. Guan,²² A. Q. Guo,^{31,62} L. B. Guo,⁴¹ M. J. Guo,⁴⁹ R. P. Guo,⁴⁸ Y. P. Guo,^{13,f} A. Guskov,^{36,a} T. T. Han,⁴⁹ W. Y. Han,³⁹ X. Q. Hao,¹⁹ F. A. Harris,⁶⁴ K. K. He,⁵⁴ K. L. He,^{1,62} F. H. H. Heinsius,⁴ C. H. Heinz,³⁵ Y. K. Heng,^{1,57,62} C. Herold,⁵⁹ T. Holtmann,⁴ P. C. Hong,^{13,f} G. Y. Hou,^{1,62} X. T. Hou,^{1,62} Y. R. Hou,⁶² Z. L. Hou,¹ H. M. Hu,^{1,62} J. F. Hu,^{55,i} T. Hu,^{1,57,62} Y. Hu,¹ G. S. Huang,^{70,57} K. X. Huang,⁵⁸ L. Q. Huang,^{31,62} X. T. Huang,⁴⁹ Y. P. Huang,¹ T. Hussain,⁷² N. Hüsken,^{27,35} W. Imoehl,²⁷ J. Jackson,²⁷ S. Jaeger,⁴ S. Janchiv,³² J. H. Jeong,¹¹ Q. Ji,¹ Q. P. Ji,¹⁹ X. B. Ji,^{1,62} X. L. Ji,^{1,57} Y. Y. Ji,⁴⁹ X. Q. Jia,⁴⁹ Z. K. Jia,^{70,57} H. J. Jiang,⁷⁵ P. C. Jiang,^{46,g} S. S. Jiang,³⁹ T. J. Jiang,¹⁶ X. S. Jiang,^{1,57,62} Y. Jiang,^{70,57} Y. Jiang,⁶² J. B. Jiao,⁴⁹ Z. Jiao,²³ S. Jin,⁴² Y. Jin,⁶⁵ M. Q. Jing,^{1,62} T. Johansson,⁷⁴ X. K.,¹ S. Kabana,³³ N. Kalantar-Nayestanaki,⁶³ X. L. Kang,¹⁰ X. S. Kang,⁴⁰ M. Kavatsyuk,⁶³ B. C. Ke,⁸⁰ A. Khoukaz,⁶⁷ R. Kiuchi,¹ R. Kliemt,¹⁴ O. B. Kolcu,^{61a} B. Kopf,⁴ M. Kuessner,⁴ A. Kupsc,^{44,74} W. Kühn,³⁷ J. J. Lane,⁶⁶ P. Larin,¹⁸ A. Lavanaia,²⁶ L. Lavezzi,^{73a,73c} T. T. Lei,^{70,57} Z. H. Lei,^{70,57} H. Leithoff,³⁵ M. Lellmann,³⁵ T. Lenz,³⁵ C. Li,⁴³ C. Li,⁴⁷ C. H. Li,³⁹ Cheng Li,^{70,57} D. M. Li,⁸⁰ F. Li,^{1,57} G. Li,¹ H. Li,^{70,57} H. B. Li,^{1,62} H. J. Li,¹⁹ H. N. Li,^{55,i} Hui Li,⁴³ J. R. Li,⁶⁰ J. S. Li,⁵⁸ J. W. Li,⁴⁹ K. L. Li,¹⁹ Ke Li,¹ L. J. Li,^{1,62} L. K. Li,¹ Lei Li,³ M. H. Li,⁴³ P. R. Li,^{38,j,k} Q. X. Li,⁴⁹ S. X. Li,¹³ T. Li,⁴⁹ W. D. Li,^{1,62} W. G. Li,¹ X. H. Li,^{70,57} X. L. Li,⁴⁹ Xiaoyu Li,^{1,62} Y. G. Li,^{46,g} Z. J. Li,⁵⁸ C. Liang,⁴² H. Liang,^{70,57} H. Liang,³⁴ H. Liang,^{1,62} Y. F. Liang,⁵³ Y. T. Liang,^{31,62} G. R. Liao,¹⁵ L. Z. Liao,⁴⁹ Y. P. Liao,^{1,62} J. Libby,²⁶ A. Limphirat,⁵⁹ D. X. Lin,^{31,62} T. Lin,¹ B. J. Liu,¹ B. X. Liu,⁷⁵ C. Liu,³⁴ C. X. Liu,¹ F. H. Liu,⁵² Fang Liu,¹ Feng Liu,⁷ G. M. Liu,^{55,i} H. Liu,^{38,j,k} H. M. Liu,^{1,62} Huanhuan Liu,¹ Huihui Liu,²¹ J. B. Liu,^{70,57} J. L. Liu,⁷¹ J. Y. Liu,^{1,62} K. Liu,¹ K. Y. Liu,⁴⁰ Ke Liu,²² L. Liu,^{70,57} L. C. Liu,⁴³ Lu Liu,⁴³ M. H. Liu,^{13,f} P. L. Liu,¹ Q. Liu,⁶² S. B. Liu,^{70,57} T. Liu,^{13,f} W. K. Liu,⁴³ W. M. Liu,^{70,57} X. Liu,^{38,j,k} Y. Liu,^{38,j,k} Y. Liu,⁸⁰ Y. B. Liu,⁴³ Z. A. Liu,^{1,57,62} Z. Q. Liu,⁴⁹ X. C. Lou,^{1,57,62} F. X. Lu,⁵⁸ H. J. Lu,²³ J. G. Lu,^{1,57} X. L. Lu,¹ Y. Lu,⁸ Y. P. Lu,^{1,57} Z. H. Lu,^{1,62} C. L. Luo,⁴¹ M. X. Luo,⁷⁹ T. Luo,^{13,f} X. L. Luo,^{1,57} X. R. Lyu,⁶² Y. F. Lyu,⁴³ F. C. Ma,⁴⁰ H. L. Ma,¹ J. L. Ma,^{1,62} L. L. Ma,⁴⁹ M. M. Ma,^{1,62} Q. M. Ma,¹ R. Q. Ma,^{1,62} R. T. Ma,⁶² X. Y. Ma,^{1,57} Y. Ma,^{46,g} Y. M. Ma,³¹ F. E. Maas,¹⁸ M. Maggiora,^{73a,73c} S. Malde,⁶⁸ Q. A. Malik,⁷² A. Mangoni,^{28b} Y. J. Mao,^{46,g} Z. P. Mao,¹ S. Marcello,^{73a,73c} Z. X. Meng,⁶⁵ J. G. Messchendorp,^{14,63} G. Mezzadri,^{29a} H. Miao,^{1,62} T. J. Min,⁴² R. E. Mitchell,²⁷ X. H. Mo,^{1,57,62} N. Yu. Muchnoi,^{5,b} J. Muskalla,³⁵ Y. Nefedov,³⁶ F. Nerling,^{18,d} I. B. Nikolaev,^{5,b} Z. Ning,^{1,57} S. Nisar,^{12,1} W. D. Niu,⁵⁴ Y. Niu,⁴⁹ S. L. Olsen,⁶² Q. Ouyang,^{1,57,62} S. Pacetti,^{28b,28c} X. Pan,⁵⁴ Y. Pan,⁵⁶ A. Pathak,³⁴ P. Patteri,^{28a} Y. P. Pei,^{70,57} M. Pelizaeus,⁴ H. P. Peng,^{70,57} K. Peters,^{14,d} J. L. Ping,⁴¹ R. G. Ping,^{1,62} S. Plura,³⁵ S. Pogodin,³⁶ V. Prasad,³³ F. Z. Qi,¹ H. Qi,^{70,57} H. R. Qi,⁶⁰ M. Qi,⁴² T. Y. Qi,^{13,f} S. Qian,^{1,57} W. B. Qian,⁶² C. F. Qiao,⁶² J. J. Qin,⁷¹ L. Q. Qin,¹⁵ X. P. Qin,^{13,f} X. S. Qin,⁴⁹ Z. H. Qin,^{1,57} J. F. Qiu,¹ S. Q. Qu,⁶⁰ C. F. Redmer,³⁵ K. J. Ren,³⁹ A. Rivetti,^{73c} M. Rolo,^{73c} G. Rong,^{1,62} Ch. Rosner,¹⁸ S. N. Ruan,⁴³ N. Salone,⁴⁴ A. Sarantsev,^{36,c} Y. Schelhaas,³⁵ K. Schoenning,⁷⁴ M. Scodreggio,^{29a,29b} K. Y. Shan,^{13,f} W. Shan,²⁴ X. Y. Shan,^{70,57} J. F. Shangguan,⁵⁴ L. G. Shao,^{1,62} M. Shao,^{70,57} C. P. Shen,^{13,f} H. F. Shen,^{1,62} W. H. Shen,⁶² X. Y. Shen,^{1,62} B. A. Shi,⁶² H. C. Shi,^{70,57} J. L. Shi,¹³ J. Y. Shi,¹ Q. Q. Shi,⁵⁴ R. S. Shi,^{1,62} X. Shi,^{1,57} J. J. Song,¹⁹ T. Z. Song,⁵⁸ W. M. Song,^{34,1} Y. J. Song,¹³ Y. X. Song,^{46,g} S. Sosio,^{73a,73c} S. Spataro,^{73a,73c} F. Stierler,³⁵ Y. J. Su,⁶² G. B. Sun,⁷⁵ G. X. Sun,¹ H. Sun,⁶² H. K. Sun,¹ J. F. Sun,¹⁹ K. Sun,⁶⁰ L. Sun,⁷⁵ S. S. Sun,^{1,62} T. Sun,^{1,62} W. Y. Sun,³⁴ Y. Sun,¹⁰ Y. J. Sun,^{70,57} Y. Z. Sun,¹ Z. T. Sun,⁴⁹ Y. X. Tan,^{70,57} C. J. Tang,⁵³ G. Y. Tang,¹ J. Tang,⁵⁸ Y. A. Tang,⁷⁵ L. Y. Tao,⁷¹ Q. T. Tao,^{25,h} M. Tat,⁶⁸ J. X. Teng,^{70,57} V. Thoren,⁷⁴ W. H. Tian,⁵¹ W. H. Tian,⁵⁸ Y. Tian,^{31,62} Z. F. Tian,⁷⁵ I. Uman,^{61b}

S. J. Wang,⁴⁹ B. Wang,¹ B. L. Wang,⁶² Bo Wang,^{70,57} C. W. Wang,⁴² D. Y. Wang,^{46,g} F. Wang,⁷¹ H. J. Wang,^{38,j,k}
H. P. Wang,^{1,62} J. P. Wang,⁴⁹ K. Wang,^{1,57} L. L. Wang,¹ M. Wang,⁴⁹ Meng Wang,^{1,62} S. Wang,^{13,f} S. Wang,^{38,j,k} T. Wang,^{13,f}
T. J. Wang,⁴³ W. Wang,⁵⁸ W. Wang,⁷¹ W. P. Wang,^{35,18,70,57} X. Wang,^{46,g} X. F. Wang,^{38,j,k} X. J. Wang,³⁹ X. L. Wang,^{13,f}
Y. Wang,⁶⁰ Y. D. Wang,⁴⁵ Y. F. Wang,^{1,57,62} Y. H. Wang,⁴⁷ Y. N. Wang,⁴⁵ Y. Q. Wang,¹ Yaqian Wang,^{17,1} Yi Wang,⁶⁰
Z. Wang,^{1,57} Z. L. Wang,⁷¹ Z. Y. Wang,^{1,62} Ziyi Wang,⁶² D. Wei,⁶⁹ D. H. Wei,¹⁵ F. Weidner,⁶⁷ S. P. Wen,¹ C. W. Wenzel,⁴
U. Wiedner,⁴ G. Wilkinson,⁶⁸ M. Wolke,⁷⁴ L. Wollenberg,⁴ C. Wu,³⁹ J. F. Wu,^{1,62} L. H. Wu,¹ L. J. Wu,^{1,62} X. Wu,^{13,f}
X. H. Wu,³⁴ Y. Wu,⁷⁰ Y. H. Wu,⁵⁴ Y. J. Wu,³¹ Z. Wu,^{1,57} L. Xia,^{70,57} X. M. Xian,³⁹ T. Xiang,^{46,g} D. Xiao,^{38,j,k} G. Y. Xiao,⁴²
S. Y. Xiao,¹ Y. L. Xiao,^{13,f} Z. J. Xiao,⁴¹ C. Xie,⁴² X. H. Xie,^{46,g} Y. Xie,⁴⁹ Y. G. Xie,^{1,57} Y. H. Xie,⁷ Z. P. Xie,^{70,57}
T. Y. Xing,^{1,62} C. F. Xu,^{1,62} C. J. Xu,⁵⁸ G. F. Xu,¹ H. Y. Xu,⁶⁵ Q. J. Xu,¹⁶ Q. N. Xu,³⁰ W. Xu,^{1,62} W. L. Xu,⁶⁵ X. P. Xu,⁵⁴
Y. C. Xu,⁷⁷ Z. P. Xu,⁴² Z. S. Xu,⁶² F. Yan,^{13,f} L. Yan,^{13,f} W. B. Yan,^{70,57} W. C. Yan,⁸⁰ X. Q. Yan,¹ H. J. Yang,^{50,e} H. L. Yang,³⁴
H. X. Yang,¹ Tao Yang,¹ Y. Yang,^{13,f} Y. F. Yang,⁴³ Y. X. Yang,^{1,62} Yifan Yang,^{1,62} Z. W. Yang,^{38,j,k} Z. P. Yao,⁴⁹ M. Ye,^{1,57}
M. H. Ye,⁹ J. H. Yin,¹ Z. Y. You,⁵⁸ B. X. Yu,^{1,57,62} C. X. Yu,⁴³ G. Yu,^{1,62} J. S. Yu,^{25,h} T. Yu,⁷¹ X. D. Yu,^{46,g} C. Z. Yuan,^{1,62}
L. Yuan,² S. C. Yuan,¹ X. Q. Yuan,¹ Y. Yuan,^{1,62} Z. Y. Yuan,⁵⁸ C. X. Yue,³⁹ A. A. Zafar,⁷² F. R. Zeng,⁴⁹ X. Zeng,^{13,f}
Y. Zeng,^{25,h} Y. J. Zeng,^{1,62} X. Y. Zhai,³⁴ Y. C. Zhai,⁴⁹ Y. H. Zhan,⁵⁸ A. Q. Zhang,^{1,62} B. L. Zhang,^{1,62} B. X. Zhang,¹
D. H. Zhang,⁴³ G. Y. Zhang,¹⁹ H. Zhang,⁷⁰ H. H. Zhang,³⁴ H. H. Zhang,⁵⁸ H. Q. Zhang,^{1,57,62} H. Y. Zhang,^{1,57} J. Zhang,⁸⁰
J. J. Zhang,⁵¹ J. L. Zhang,²⁰ J. Q. Zhang,⁴¹ J. W. Zhang,^{1,57,62} J. X. Zhang,^{38,j,k} J. Y. Zhang,¹ J. Z. Zhang,^{1,62} Jianyu Zhang,⁶²
Jiawei Zhang,^{1,62} L. M. Zhang,⁶⁰ L. Q. Zhang,⁵⁸ Lei Zhang,⁴² P. Zhang,^{1,62} Q. Y. Zhang,^{39,80} Shuihan Zhang,^{1,62}
Shulei Zhang,^{25,h} X. D. Zhang,⁴⁵ X. M. Zhang,¹ X. Y. Zhang,⁴⁹ Xuyan Zhang,⁵⁴ Y. Zhang,⁷¹ Y. Zhang,⁶⁸ Y. T. Zhang,⁸⁰
Y. H. Zhang,^{1,57} Yan Zhang,^{70,57} Yao Zhang,¹ Z. H. Zhang,¹ Z. L. Zhang,³⁴ Z. Y. Zhang,⁴³ Z. Y. Zhang,⁷⁵ G. Zhao,¹ J. Zhao,³⁹
J. Y. Zhao,^{1,62} J. Z. Zhao,^{1,57} Lei Zhao,^{70,57} Ling Zhao,¹ M. G. Zhao,⁴³ S. J. Zhao,⁸⁰ Y. B. Zhao,^{1,57} Y. X. Zhao,^{31,62}
Z. G. Zhao,^{70,57} A. Zhemchugov,^{36,a} B. Zheng,⁷¹ J. P. Zheng,^{1,57} W. J. Zheng,^{1,62} Y. H. Zheng,⁶² B. Zhong,⁴¹ X. Zhong,⁵⁸
H. Zhou,⁴⁹ L. P. Zhou,^{1,62} X. Zhou,⁷⁵ X. K. Zhou,⁷ X. R. Zhou,^{70,57} X. Y. Zhou,³⁹ Y. Z. Zhou,^{13,f} J. Zhu,⁴³ K. Zhu,¹
K. J. Zhu,^{1,57,62} L. Zhu,³⁴ L. X. Zhu,⁶² S. H. Zhu,⁶⁹ S. Q. Zhu,⁴² T. J. Zhu,^{13,f} W. J. Zhu,^{13,f} Y. C. Zhu,^{70,57} Z. A. Zhu,^{1,62}
J. H. Zou,¹ and J. Zu^{70,57}

(BESIII Collaboration)

¹*Institute of High Energy Physics, Beijing 100049, People's Republic of China*²*Beihang University, Beijing 100191, People's Republic of China*³*Beijing Institute of Petrochemical Technology, Beijing 102617, People's Republic of China*⁴*Bochum Ruhr-University, D-44780 Bochum, Germany*⁵*Budker Institute of Nuclear Physics SB RAS (BINP), Novosibirsk 630090, Russia*⁶*Carnegie Mellon University, Pittsburgh, Pennsylvania 15213, USA*⁷*Central China Normal University, Wuhan 430079, People's Republic of China*⁸*Central South University, Changsha 410083, People's Republic of China*⁹*China Center of Advanced Science and Technology, Beijing 100190, People's Republic of China*¹⁰*China University of Geosciences, Wuhan 430074, People's Republic of China*¹¹*Chung-Ang University, Seoul, 06974, Republic of Korea*¹²*COMSATS University Islamabad, Lahore Campus, Defence Road, Off Raiwind Road, 54000 Lahore, Pakistan*¹³*Fudan University, Shanghai 200433, People's Republic of China*¹⁴*GSI Helmholtzcentre for Heavy Ion Research GmbH, D-64291 Darmstadt, Germany*¹⁵*Guangxi Normal University, Guilin 541004, People's Republic of China*¹⁶*Hangzhou Normal University, Hangzhou 310036, People's Republic of China*¹⁷*Hebei University, Baoding 071002, People's Republic of China*¹⁸*Helmholtz Institute Mainz, Staudinger Weg 18, D-55099 Mainz, Germany*¹⁹*Henan Normal University, Xinxiang 453007, People's Republic of China*²⁰*Henan University, Kaifeng 475004, People's Republic of China*²¹*Henan University of Science and Technology, Luoyang 471003, People's Republic of China*²²*Henan University of Technology, Zhengzhou 450001, People's Republic of China*²³*Huangshan College, Huangshan 245000, People's Republic of China*²⁴*Hunan Normal University, Changsha 410081, People's Republic of China*²⁵*Hunan University, Changsha 410082, People's Republic of China*²⁶*Indian Institute of Technology Madras, Chennai 600036, India*

- ²⁷Indiana University, Bloomington, Indiana 47405, USA
- ^{28a}INFN Laboratori Nazionali di Frascati, I-00044, Frascati, Italy
- ^{28b}INFN Sezione di Perugia, I-06100, Perugia, Italy
- ^{28c}University of Perugia, I-06100, Perugia, Italy
- ^{29a}INFN Sezione di Ferrara, I-44122, Ferrara, Italy
- ^{29b}University of Ferrara, I-44122, Ferrara, Italy
- ³⁰Inner Mongolia University, Hohhot 010021, People's Republic of China
- ³¹Institute of Modern Physics, Lanzhou 730000, People's Republic of China
- ³²Institute of Physics and Technology, Peace Avenue 54B, Ulaanbaatar 13330, Mongolia
- ³³Instituto de Alta Investigación, Universidad de Tarapacá, Casilla 7D, Arica 1000000, Chile
- ³⁴Jilin University, Changchun 130012, People's Republic of China
- ³⁵Johannes Gutenberg University of Mainz, Johann-Joachim-Becher-Weg 45, D-55099 Mainz, Germany
- ³⁶Joint Institute for Nuclear Research, 141980 Dubna, Moscow region, Russia
- ³⁷Justus-Liebig-Universität Giessen, II. Physikalisches Institut, Heinrich-Buff-Ring 16, D-35392 Giessen, Germany
- ³⁸Lanzhou University, Lanzhou 730000, People's Republic of China
- ³⁹Liaoning Normal University, Dalian 116029, People's Republic of China
- ⁴⁰Liaoning University, Shenyang 110036, People's Republic of China
- ⁴¹Nanjing Normal University, Nanjing 210023, People's Republic of China
- ⁴²Nanjing University, Nanjing 210093, People's Republic of China
- ⁴³Nankai University, Tianjin 300071, People's Republic of China
- ⁴⁴National Centre for Nuclear Research, Warsaw 02-093, Poland
- ⁴⁵North China Electric Power University, Beijing 102206, People's Republic of China
- ⁴⁶Peking University, Beijing 100871, People's Republic of China
- ⁴⁷Qufu Normal University, Qufu 273165, People's Republic of China
- ⁴⁸Shandong Normal University, Jinan 250014, People's Republic of China
- ⁴⁹Shandong University, Jinan 250100, People's Republic of China
- ⁵⁰Shanghai Jiao Tong University, Shanghai 200240, People's Republic of China
- ⁵¹Shanxi Normal University, Linfen 041004, People's Republic of China
- ⁵²Shanxi University, Taiyuan 030006, People's Republic of China
- ⁵³Sichuan University, Chengdu 610064, People's Republic of China
- ⁵⁴Soochow University, Suzhou 215006, People's Republic of China
- ⁵⁵South China Normal University, Guangzhou 510006, People's Republic of China
- ⁵⁶Southeast University, Nanjing 211100, People's Republic of China
- ⁵⁷State Key Laboratory of Particle Detection and Electronics, Beijing 100049, Hefei 230026, People's Republic of China
- ⁵⁸Sun Yat-Sen University, Guangzhou 510275, People's Republic of China
- ⁵⁹Suranaree University of Technology, University Avenue 111, Nakhon Ratchasima 30000, Thailand
- ⁶⁰Tsinghua University, Beijing 100084, People's Republic of China
- ^{61a}Turkish Accelerator Center Particle Factory Group, Istinye University, 34010, Istanbul, Turkey
- ^{61b}Near East University, Nicosia, North Cyprus, 99138, Mersin 10, Turkey
- ⁶²University of Chinese Academy of Sciences, Beijing 100049, People's Republic of China
- ⁶³University of Groningen, NL-9747 AA Groningen, The Netherlands
- ⁶⁴University of Hawaii, Honolulu, Hawaii 96822, USA
- ⁶⁵University of Jinan, Jinan 250022, People's Republic of China
- ⁶⁶University of Manchester, Oxford Road, Manchester, M13 9PL, United Kingdom
- ⁶⁷University of Muenster, Wilhelm-Klemm-Strasse 9, 48149 Muenster, Germany
- ⁶⁸University of Oxford, Keble Road, Oxford OX13RH, United Kingdom
- ⁶⁹University of Science and Technology Liaoning, Anshan 114051, People's Republic of China
- ⁷⁰University of Science and Technology of China, Hefei 230026, People's Republic of China
- ⁷¹University of South China, Hengyang 421001, People's Republic of China
- ⁷²University of the Punjab, Lahore-54590, Pakistan
- ^{73a}University of Turin and INFN, University of Turin, I-10125, Turin, Italy
- ^{73b}University of Eastern Piedmont, I-15121, Alessandria, Italy
- ^{73c}INFN, I-10125, Turin, Italy
- ⁷⁴Uppsala University, Box 516, SE-75120 Uppsala, Sweden
- ⁷⁵Wuhan University, Wuhan 430072, People's Republic of China
- ⁷⁶Xinyang Normal University, Xinyang 464000, People's Republic of China
- ⁷⁷Yantai University, Yantai 264005, People's Republic of China
- ⁷⁸Yunnan University, Kunming 650500, People's Republic of China

⁷⁹*Zhejiang University, Hangzhou 310027, People's Republic of China*
⁸⁰*Zhengzhou University, Zhengzhou 450001, People's Republic of China*

^aAlso at the Moscow Institute of Physics and Technology, Moscow 141700, Russia.

^bAlso at the Novosibirsk State University, Novosibirsk, 630090, Russia.

^cAlso at the NRC “Kurchatov Institute,” PNPI, 188300, Gatchina, Russia.

^dAlso at Goethe University Frankfurt, 60323 Frankfurt am Main, Germany.

^eAlso at Key Laboratory for Particle Physics, Astrophysics and Cosmology, Ministry of Education; Shanghai Key Laboratory for Particle Physics and Cosmology; Institute of Nuclear and Particle Physics, Shanghai 200240, People's Republic of China.

^fAlso at Key Laboratory of Nuclear Physics and Ion-beam Application (MOE) and Institute of Modern Physics, Fudan University, Shanghai 200443, People's Republic of China.

^gAlso at State Key Laboratory of Nuclear Physics and Technology, Peking University, Beijing 100871, People's Republic of China.

^hAlso at School of Physics and Electronics, Hunan University, Changsha 410082, China.

ⁱAlso at Guangdong Provincial Key Laboratory of Nuclear Science, Institute of Quantum Matter, South China Normal University, Guangzhou 510006, China.

^jAlso at Frontiers Science Center for Rare Isotopes, Lanzhou University, Lanzhou 730000, People's Republic of China.

^kAlso at Lanzhou Center for Theoretical Physics, Lanzhou University, Lanzhou 730000, People's Republic of China.

^lAlso at the Department of Mathematical Sciences, IBA, Karachi 75270, Pakistan.